Multiscale segmentation and classification of remote sensing imagery with advanced edge and scale-space features

Angelos Tzotsos[a,*], Konstantinos Karantzalos[a], Demetre Argialas[a]

[a]*National Technical University of Athens, Remote Sensing Laboratory, Athens, Greece*

Abstract

The objective of this research was the development of a multiscale object-oriented image analysis framework, which incorporated a region merging segmentation algorithm enchanced by advanced edge features and nonlinear scale space filtering. For the region merging procedure the MSEG algorithm was extended, since it provided a multiscale approach. Initialy, edge and line features were extracted from remote sensing imagery at several scales using scale-space representations. The derived features were used by the enchanced segmentation algorithm as constraints for the growth of image objects at coresponding scales. The first primitive object representation was the single image pixel. Through iterative pairwise object merging, done at several iterations, the final segmentation was achieved. The borders of the images were not permitted to intersect with the egde features thus primitive objects were bounded by the edge features. Image objects were computed at various scales and were connected to a kernel-based learning machine for the classification of various earth-observation data. This approach does not require the tuning of any parameter − of those which control the edge feature extraction and multi-scale segmentation, like standard deviation, shape, color, texture etc. − since the scale hierarchy is implicitly derived from scale space representation properties. The developed object-oriented image classification framework was applied on a number of remote sensing data from different airborne and spaceborne sensors including very high resolution panchromatic, multispectral, hyperspectral aerial and satellite datasets. The very promising experimental results along with the performed qualitative and quantitative evaluation demonstrate the potential of the proposed approach.

Keywords: Object-Based Image Analysis, Anisotropic Diffusion, Line Features, Region Merging, Machine Learning

*Corresponding author. Tel.: +30 210 7722684. Fax.: +30 210 7722594. Address: Heroon Polytechniou 9, Zographos, 15780, Greece

Email addresses: tzotsos@gmail.com (Angelos Tzotsos), karank@central.ntua.gr (Konstantinos Karantzalos), argialas@central.ntua.gr (Demetre Argialas)

1. Introduction

The current need for automated image analysis and computer vision technological tools require a processing scheme able to encapsulate effectively the content of remote sensing data. However, earth's landscape structure is complex, the context varies and so does the appearance of the images being a combination of many different intensities, representing natural features such as vegetation, geomorphological and hydrological features, man-made objects (e.g buildings, roads) and artefacts caused by variation in illumination of the terrain (e.g shadows).

Furthermore, roads, infrastructure, vegetation, landforms and other land features appear in different sizes and geographical scales in images (e.g. country road versus interstate, tree stands versus forest, maisonette versus polygon building, rill versus river, etc). Only in a few special circumstances the objects of interest belong to a certain scale while the remaining ones, to be discarded, to another. In most cases such a global scale threshold is not possible since the desired information is present at several scales (Witkin, 1983; Lindeberg, 1994; Weickert, 1998; Meyer and Maragos, 2000).

Therefore, scale space representations and multiscale image analysis provide the framework to explore the entire image content by detecting the scale(s) at which objects or patterns appear and are most distinctly identified. Towards this end and in a similar way to the human visual system, several multiscale low level processing approaches (i.e. filtering, segmentation, etc) have been developed during which a series of coarser and coarser representations of the same image are computed and used for the recognition of image objects (Blaschke and Hay, 2001; Hay et al., 2002; Hall and Hay, 2003; Benz et al., 2004; Stewart et al., 2004; Jimenez et al., 2005; Karantzalos and Argialas, 2006; Duarte Carvajalino et al., 2008; Ouma et al., 2008). The mathematical models and the manner for constructing these scale space representations is of fundamental importance.

In addition, during the last decade the way of classifying remote sensing is been changing and instead of classifying individual pixels into discrete land cover classes, object-based classification approaches construct a hierarchical object representation of an image and the classifier is responsible for associating them with a land cover class (Blaschke, 2010). Therefore, it is not just the spectral signature of each pixel, but the statistical, geometric and topological characteristics of each object that play a key role during classification. Recent studies are highlighting that the determination of one or more optimal filtering scales for image segmentation is still a challenge and that a multiscale object-based classification is a significantly better approach than the classical per-pixel classification procedure (Myint et al., 2011; Tzotsos et al., 2011).

In this chapter, we propose an object-based image analysis framework which integrates advanced scale space representations, edge and line feature detection, multiscale segmentation and a kernel-based classification. The contributions of our approach are twofold. We introduce:

- a generic framework able to process any remote sensing data (high/ very high resolution satellite/airborne data, multispectral/ hyperspectral data and radar data) without the need of tuning any parameter (scale, color, texture, etc) and
- a robust multi-scale segmentation procedure which is constrained by advanced edge-based features

The remainder of the paper is structured as follows. In Section 2, the related work on scale space representations, multiscale object-based analysis and edge-based image segmentation are briefly reviewed. The developed object-based image analysis framework is detailed in Section 3, along with a description and detailed analysis of its different processing steps. Experimental results and the performed quantitative evaluation are given in Section 4. Finally, conclusions and perspectives for future work are in Section 5.

2. Related Work

2.1. Multiscale object-based image analysis

Along with the gradual availability of earth observation data with higher spatial and spectral resolution, research efforts in classifying remote sensing data have been shifting in the last decade from pixel-based approaches to object-based ones (Blaschke, 2010: Myint et al., 2011; Tzotsos et al., 2011). Assigning land cover classes to individual pixels can be intuitively proper and functional for low resolution data. However, this is not the case for the emerging applications which arise from the continuously improving remote sensing sensors (Aplin and Smith, 2008; Blaschke et al., 2008). This is mostly because at higher resolutions it is a connected group of pixels that is likely to be associated with a land cover class and not just an individual pixel (Tzotsos et al., 2011).

In addition, the earth surface exhibits various regular and irregular structures which are represented with a certain spatial heterogeneity in images composing their intensity, scale and texture. Several important aspects of earth observation data can not be analyzed based on pixel information, but can only be exploited based on contextual information and the topologic relations of the objects of interest (Liu et al., 2008) through a multiscale image analysis (Blaschke and Hay, 2001; Hay et al., 2002; Hall and Hay, 2003; Benz et al., 2004; Stewart et al., 2004; Jimenez et al., 2005; Duarte Carvajalino et al., 2008; Ouma et al., 2008; Tzotsos et al., 2011). Starting with the observed spatial heterogeneity and variability, meaningful spatial aggregations (objects) can be formed at certain image scales configuring a relationship between ground objects and image objects. With such an object-based multiscale analysis, which is based on certain hierarchically structured rules, the relationship between the different scales of the spatial entities is described.

During the last decade, a number of object-based image analysis software were developed (Baatz and Schape, 2000; Tzotsos and Argialas, 2006; Inglada and Christophe, 2009; Christophe and Inglada, 2009) enabling the broad application on various engineering and environmental remote sensing studies (Benz et al., 2004; Zhou et al., 2009; Dragut et al., 2009; Blaschke, 2010; Mladinich et al., 2010). In all cases, the challenge was to construct an efficient scale-space object representation through certain multiscale (region merging or other) segmentation techniques (Blaschke et al., 2004; Carleer et al., 2005; Jimenez et al., 2005; Neubert et al., 2006; Tzotsos and Argialas, 2006), which partition the image on several regions/objects, based on the spectral homogeneity in a local neighborhood. In addition to the spectral homogeneity criterion, shape parameters are used to define geometric properties that the segmentation algorithm must take into account when computing the overall homogeneity (scale parameter) of each image object during search for optimal merges.

In 2008, a texture optimization procedure was introduced for the MSEG algorithm (Tzotsos et al., 2008) integrating grey level co-occurrence matrices and introducing an object-based cost measure for texture homogeneity as an additional parameter to the segmentation procedure. Such an integration of spatial and spectral information can produce a multiscale object representation but only through an iterative and exhaustive tuning (based on trial and error investigation) of certain parameters, like shape, scale, texture, etc. (Baatz and Schape, 2000; Benz et al., 2004; Blaschke et al., 2004; Carleer

et al., 2005; Hay et al., 2005; Tzotsos and Argialas, 2006; Ouma et al., 2008; Dragut et al., 2009; Zhou et al., 2009).

Other research efforts were based on the construction of linear scale spaces for the multiscale analysis of several landscape structures (Blaschke and Hay, 2001; Hay et al., 2003, 2002; Stewart et al., 2004) or on the reconstruction of multiscale representations through object-specific analysis and up-scaling, through the computation of a number of coarse and fine scales by sampling the initial image (Hall and Hay, 2003). Furthermore, other studies employed unsupervised classification algorithms for both optical and radar data (Derode and Mercier, 2007; Jung, 2007) or multiple hierarchical segmentations (Akcay and Aksoy, 2008).

More recent research effort are focusing on optimizing the segmentation procedure through a data-driven thresholding manner (Martha et al., 2011) and on constructing advanced nonlinear scale space representation for efficient supervised classification (Tzotsos et al., 2011) and change detection over urban areas (Doxani et al., 2012).

2.2. Scale space remote sensing data representations

Terrain objects do not belong to a single but to many scales. The use of scale space image representations is thus of fundamental importance for a number of image analysis and computer vision tasks. It dates back to sixties and was first introduced by Iijima (Weickert et al., 1999). In western literature and following the ideas of Witkin (1983), Koenderink (1984) and Lindeberg (1994), many methods were introduced to derive linear scale spaces and respectively many isotropic multiscale operators were developed. Either through Gaussian filtering or through isotropic multi-resolution analysis (by down-sampling the initial data), all linear scale space approaches present the same important drawback: image edges are blurred and new non-semantic objects may appear at coarse scales (Witkin, 1983; Paragios et al., 2005; Ouma et al., 2008). Under a hierarchical multiscale segmentation or an object-based classification framework, the thematic information to be extracted is directly related with the primitive image objects computed at every scale. The better these primitive objects represent real-world entities, the better they can describe the semantics of the image (Hay and Castilla, 2006; Blaschke et al., 2008; Hofmann et al., 2008; Tzotsos et al., 2011). Therefore, the selection of the appropriate approach for constructing the multiscale image and hierarchical object representation is of great importance.

Since linear scale space approaches, by acting isotropically in the image domain, delocalize and blur image edges, nonlinear operators and nonlinear scale spaces have been studied and applied in various image processing and computer vision applications. Following the pioneering work of Perona and Malik (1990) there has been a flurry of activity in partial differential equation and anisotropic diffusion filtering techniques (Weickert, 1998). For remote sensing applications, a number of anisotropic diffusion schemes have been proposed and applied to aerial and satellite datasets (Lennon et al., 2002; Camps-valls and Bruzzone, 2005; Karantzalos and Argialas, 2006; Duarte-Carvajalino et al., 2007; Ouma et al., 2008; Plaza et al., 2009), combined, in most cases, with pixel-based classification techniques. All their scale space formulations, though, were based either on diffusions during which the average luminance value is preserved or on geometrically driven ones formulated

under a variational framework. Although these formulations may reduce the problems of isotropic filtering, they do not eliminate them completely: spurious extrema and important intensity shifts may still appear (Meyer and Maragos, 2000; Karantzalos et al., 2007; Tzotsos et al., 2011).

Therefore, another way to produce nonlinear scale spaces is through mathematical morphology and, in particular, with morphological levelings, which have been introduced by Meyer (1998) and further studied by Matheron (1997) and Serra (2000). Morphological levelings overcome the drawback of spurious extrema or important intensity shifts and possess a number of desired properties for the construction of elegant scale space representations. Levelings, which are a general class of self-dual morphological operators, do not displace contours through scales and are characterized by a number of desirable properties for the construction of nonlinear scale space representations. They satisfy the following spatial and spectral properties/axioms (Meyer and Maragos, 2000; Meyer, 2004; Karantzalos et al., 2007; Tzotsos et al., 2011):

- invariance by spatial translation,
- isotropy, invariance by rotation,
- invariance to a change of illumination,
- the causality principle,
- the maximum principle, excluding the extreme case where g is completely flat.

In addition, levelings:

- do not produce new extrema at larger scales,
- enlarge smooth zones,
- they also create new smooth zones
- they are particularly robust (strong morphological filters)
- they do not displace edges

Designing and formulating an optimal scale space framework in still an active area of research. Studies on certain scale space formulation Duanggate-ctal:11,Nilufar-ctal:12,Ouzounis-ctal:12, studies on a varying stopping time (Gilboa, 2008) and on the behavior on corner and other local descriptors (Zhong et al., 2009; Jiang et al., 2011; Kimmel et al., 2011; Xu et al., 2012) are recent efforts.

2.3. Edge-based segmentation

Extracting primitives (i.e. contours, edges, lines, etc) is a basic low-level operation in the human visual system. Along with our aim to understand and simulate the human vision, the importance of building up computational models for the perception of primitives is a major component in many applications of computer vision, such as object/pattern recognition, robot vision, remote sensing and medical image analysis.

These primitives give important information about the geometric content of images. Most of the terrain objects and in particular most man-made

objects are made of flat surfaces with certain geometric features. In addition, many shapes can be described roughly or in detail with edge and line primitives. Therefore, edge or line segments can be used as a low-level feature description in order to extract information from images and can serve as the basic tool to analyze and detect more complex shapes (Von Gioi et al., 2010; Papari and Petkov, 2011: Wang and Oliensis, 2010; Chia et al., 2012). In the context of scale space representations, image primitives may support more stable and efficient representations since their description can be more independent of the object size. Moreover, defined mainly by the object geometrical properties they allow the robust and efficient feature comparison in various scales. The later is of major importance due to large appearance variations of object instances belonging to the same class.

However, even the recent more sophisticated edge and line detectors cannot produce connected segments and suffer from the terrain complexity pictured in images, shadows, occlusions, etc. Therefore, recent efforts are trying to merge the advantages of edge/line detection and image segmentation techniques in order to produce connected object contours/boundaries and a comprehensive object description (Pavlidis and Liow, 1990; Kermad and Chehdi, 2002; Cufi et al., 2003). Certain primitive combinations have been proposed in order to describe more efficiently object boundaries (Chia et al., 2012; Klonus et al., 2012). Another recent study proposed a region-based unsupervised segmentation and classification algorithm which included the computation of an edge strength model (Yu et al., 2012). This edge penalty model improved segmentation performance by preserving segment boundaries.

3. Methodology

The main objective, here, was to design the overall framework in order to be generic, robust and able to process effectively a wide variety of remote sensing data, such as hyperspectral and multispectral data from ground, aerial and spaceborne sensors, radar data, digital elevation models, etc. It is based upon the Object-Based Image Analysis (OBIA) approach, which generally includes low, medium and high level image processing sub-tasks:

- Preprocessing steps (geometric and radiometric corrections, filtering, scale space image simplification, edge detection, band math expression computations, etc.),
- Image Segmentation (in order to produce single-level or multi-level hierarchies of primitive objects within the image space),
- Computation of image object properties based on spectral, shape, topological and context features,
- Classification (learning techniques or rule-based systems to perform the classification task),
- Vectorization steps (create the output to spatial databases and integrate the information to thematic maps).

The developed approach is integrating certain computer vision and machine learning methods for implementing the above tasks. The supported type of the imagery can be up to double precision and of any number of bands. Briefly the developed framework consists of the following steps: Firstly, for

every band of the initial image, a scale-space representation is generated, using the Anisotropic Morphological Leveling (AML) formulation (Karantzalos et al., 2007). A feature extraction step is then applied on the scale-space stack. For this step two algorithms were tested and are presented here: the Canny edge detector (Canny, 1986) and the Line Segment Detector (LSD) (Von Gioi et al., 2010). A multi-scale segmentation algorithm is applied afterwards which is able to integrate the simplified scale space stack along with the corresponding edge information. During this step primitive image objects are formed. The procedure starts from single-pixel, and through pair-wise merges bounded by edge information, several levels of image objects are produced. The multiscale object hierarchies is been constructed without any parameter tuning. In a similar way with (Tzotsos et al., 2011), here the edge features are produced without tuning the edge extraction parameters (Fig. 1). Last in the processing order comes a dual classification procedure using a support vector machine classifier. The first classification is performed on all scale-space representations and their corresponding segmentations, while the second optimal one is performed after an interim accuracy assessment.

3.1. Scale-Space Filtering

The first step in the developed approach is the construction of the non-linear scale-space representation in order to elegantly simplify raw data. Anisotropic diffusion methods are used widely in computer vision applications to simulate the filtering procedures that are performed in the human vision system. Such methods provide robust simplification of images without the loss of important information such as edges, that are of high importance for higher level processing algorithms. Especially in OBIA applications.

where very high resolution data are usually processed, it is very important to simplify the complexity of the initial data and provide a multiscale representation, since different features of the image reside in different scales.

For this preproccesing step, the Anisotropic Morphological Levelings (AML) (Karantzalos et al., 2007) was incorporated in the processing scheme. Anisotropic Morphological Levelings are a combination of morphological levelings with anisotropic markers and are employed in order to achieve better segmentation results, reduces the heterogeneity of image data, create accurate image objects and reduce over-segmentation. In Fig 1 one can observe that the scale space filtering by creating a series of simplified data leads to a multi-scale segmentation without tuning any segmentation parameters (like texture, color, shape, etc).

Starting from the initial image and for every available band, a scale-space representation was generated, using the AML formulation. Using iterative anisotropic morphological operations, and increasing scales (10,50,100,500,1000) a scale-space 3D representation was constructed from each initial band. The result of this step was a scale-space stack with simplified versions of the raw data. Note that during this process edge information was preserved in all scales, contrary to isotropic (e.g. Gaussian) filtering that loses edge information as scale increase (Fig 1).

3.2. Multiscale Segmentation based on Advanced Edge Features

Edge and line features were computed for every image in the scale space stack. Edge information was obtained from the standard Canny detector (Canny, 1986) and the recent Line Segment Detector (LSD) (Von Gioi et al., 2010, 2012).

The Canny edge detector was employed in order to provide primitive edge features that were integrated to the implemented region merging algorithm. Throughout this research, variance parameter of the Canny detector was set stable to 5. In Fig 1(e,n,s) results from the application of the Canny edge detection on scale-space images is shown. LSD is a linear-time Line Segment Detector giving subpixel accurate results. The algorithm starts by computing the level-line angle at each pixel to produce a level-line field, i.e., a unit vector field such that all vectors are tangent to the level line going through their base point. Then, this field is segmented into connected regions of pixels that share the same level-line angle up to a certain tolerance. These connected regions are called line support regions (Von Gioi et al., 2012). Each line support region (a set of pixels) is a candidate for a line segment. The principal inertial axis of the line support region is used as main rectangle direction. After examining and validating line support regions, and test that they are aligned properly, a selection of meaningful rectangles are selected as the final result. In Fig.1d the application of LSD on a very high resolution aerial scanner image is demonstrated. LSD has been designed to be automated and includes an internal filtering and simplification procedure with constant scale of 0.8.

For the multi-scale segmentation procedure, an improved version of the MSEG algorithm (Tzotsos and Argialas, 2006) was implemented. MSEG is a region-based multi-scale segmentation algorithm recently developed for object-oriented image analysis. Briefly, starting from a pixel representation it creates objects through continuous pair-wise object fusions, executed in iterations (passes). For each pass, every object is evaluated in relation with its

neighboring objects towards the optimal pair of objects adequate for fusion. In every pass, an image object can be merged only once, aiming at a balanced object growth. MSEG algorithm defines a cost function for each object merge and then implements various optimization techniques to minimize this cost. The cost function is implemented using the measure of homogeneity (color and shape) in the same way with other approaches (Baatz and Schape, 2000). The threshold of the allowed merging cost for the segmentation procedure is called scale parameter, since it implicitly dictates the area growth of the image objects. Results from the application of the MSEG algorithm are shown in Fig 1(c,h,m,r). Through this research, the parameters of the MSEG algorithm were set stable, the color parameter was set to 0.8 and the shape parameter was set to 0.2. The goal was to allow the elegantly simplified data (from the scale space stack) to control the way that image segments and objects are being created and not the region merging procedure. In particular, in a previous study (Tzotsos et al., 2011) is was shown that there is no need for tuning the segmentation parameters when the approach includes an elegant and reliable edge-preserving formulation for the scale space computation.

Furthermore, the MSEG algorithm was improved in order to be able to integrate edge information (as a constrain) during the segmentation procedure. The goal was to design a more robust and generic segmentation procedure that would be able to take into account advanced edge and line features. In particular, the region merging algorithm starts by selecting initialization points throughout the image using SPE (Start Point Estimation) module (Tzotsos and Argialas, 2006) and a queue of pixels is created in order to

be able to achieve reproducibility. Then, iterative pairwise fusions start to happen within the image space starting from single pixel objects, in a way that local heterogeneity is minimized (for color and shape criteria). During this pairwise merging of image objects, the edge information is used as a boundary. Two adjacent pixels will not be merged into an object if one of both resides on top of an edge. After the first pass of the region merging procedure, image objects of one or two pixels exist, with edge pixels being constrained and not merged to each other. During the following passes edge objects (still single pixels) are not merged, thus not permitting object merging between image regions that are separated by a line or a continuous edge feature. After several passes (iterations) converging of the algorithm occurs and no more object merging is performed, due to scale parameter. At this point the edge objects are still intact by the region merging procedure, thus binding the procedure into respecting edge features. Finally a last iteration of the algorithm is forced on edge objects only, and a selection is made, to which neighboring object they should be merged, based on local heterogeneity. This step is taking advantage to the fact that both Canny and LSD features are one-pixel wide, thus edge objects are always capable of merging with non edge objects.

A certain novelty of the developed segmentation process is that it does not use an edge penalty model for the edge compensation as presented in other approaches (Kermad and Chehdi, 2002; Cufi et al., 2003; Yu et al., 2012), but a topological constraint, effective throughout the region merging procedure. The results of this enhancement is presented in Fig. 1(e,j,o,t) showing very promising segmentation results. A scale parameter of value 100 was used

for all tests on Fig. 1, showing that scale-space representation effectively provides the scale of the obtained objects. More results are presented and discussed in following sections.

3.3. Kernel-based Classification

For the developed approach, an SVM classification scheme (Tzotsos and Argialas, 2008; Tzotsos et al., 2011) was employed. After the multiscale segmentation which is constrained by edge information, image objects were extracted and object properties were computed forming the feature space of the classification step. For each primitive image object, spectral, shape and spatial properties were extracted by the topological model used to handle object topology. This model was proposed by (Lehmann, 2008) but also developed independently in MSEG (Tzotsos and Argialas, 2006). The computed properties are bound to each object by a unique identifier within the object hierarchy of the image. Some of the objects are selected as samples and their properties formed a training set for the SVM.

The SVM classifier seeks to find the optimal separating hyperplane between classes by focusing on the training data (support vectors) that are placed at the edge of the class descriptors. Training data other than support vectors are discarded. Thus, not only an optimal hyperplane is fitted but less training samples are effectively used as well (Tzotsos and Argialas, 2008). This method works very well for classes that are linearly separable. In the case that image classes are not linearly separable, the SVM maps the feature space into a higher dimensionality using kernels (Vapnik, 1998; Theodoridis and Koutroumbas, 2003) and then separates classes in that new feature space forming the support vectors.

Since the SVM classification method was initially designed for binary classification problems, a heuristic one-against-one strategy was employed for multiclass classification (Hsu and Lin, 2002). Many binary classifiers were applied for each pair of classes and for every object of the image and then a max-win operator determined the final classification of the object. A cross validation scheme was also used in order to define the parameters needed for the training procedure. After specification of parameters, the training set was used to train the classifier. Primitive image object were classified using this trained SVM algorithm using the one-against-one strategy. Finally a quality assessment took place, using ground truth data that were not used during the training procedure.

The above classification procedure was repeated for all scales in the scale-space representation in order to determine the best classification accuracy, as proposed in (Tzotsos et al., 2011). After determining the best scale to perform classification, a final classification step took place to produce the optimal results.

To sum up, the initial dataset was simplified and a successive series of simplified images were constructed forming a nonlinear scale space. The simplified imagery that was derived was then used to extract edge and line features using advanced methods. An edge enhanced multi-scale image segmentation algorithm was employed to provide primitive image objects from the scale space images without the tuning of any standard parameter. Finally, a classification step was performed to complete the OBIA tasks and to evaluate the proposed method.

4. Evaluation and Discussion

As already stated, the overall objective of the present research was: (a) to introduce a generic and robust framework able to process any kind of remote sensing data without tuning any parameters (like scale, texture, color, etc) during the computation, (b) to introduce a multi-scale segmentation algorithm which is constrained by advanced edge-based features at various scales and (c) to evaluate the developed methodology in various remote sensing datasets.

In Fig. 1 a general overview of the proposed method is presented. Starting from the initial image (Fig. 1a), Gaussian filtering at different scales demonstrates the loss of edge information due its isotropic character (Fig.1 f,k,p). These results are directly compared with the AML scale-space representations at equivalent scales. One can observe in Fig.1 (b,g,l and q) that edge information is preserved while the initial image is simplified. For example, in the tile roof of the building the single tiles are more difficult to distinguish as scale increases. The results from the application of the standard MSEG algorithm on the simplified images using the same scale parameter value (100) are shown as well Fig.1 (c,h,m and r). The standard MSEG algorithm performs well across object boundaries but produces over-segmented results and the mean object size is increasing along with scale. The edge and line feature extraction at various scales is demonstrated in Fig.1, as well. The result from the application of the LSD in the original image is shown in Fig.1 (d). This is an impressive result, demonstrating that LSD is robust and works well for man-made objects, even if not all of the building sides have been detected correctly. The results of the Canny edge detector are

also presented at different scales Fig.1 (i,n and s). It can be observed that due to the simplified data through the AML scale space computation, more clear edge features are detected which describe accurately object boundaries. Less false detections have been, also, detected inside homogeneous regions as for example in the tile roof region. Furthermore, results from the application of the improved MSEG algorithm are presented in Fig.1 (e,j,o and t). The first result (Fig.1e) shows how the developed algorithm is constrained by the detected LSD line features. On the homogeneous regions there is not much difference which is normal since the same AML scale is used for both (c) and (e). The second result (Fig.1j) shows how the Canny edges are preserved inside the roof segments and how the improved segmentation method is been robustly constrained by edge information. This result is better than (h), where image objects are oversegmented and arbitrarily set inside a homogeneous region of the image. The third result in Fig1.(o) shows that the combination of edge information with region merging in higher scales is outperforming the standard MSEG algorithm (Fig.1m) at the same AML scale and segmentation scale parameter. Moreover, the result in Fig.1(t) shows how the scale space in combination with the edge-constrained segmentation tackles the oversegmentation issue shown in Fig.1r.

These aforementioned results demonstrate that the proposed method outperforms earlier efforts (Tzotsos and Argialas, 2008; Baatz and Schape, 2000; Tzotsos et al., 2011). In addition, in order to further validate the developed algorithm's experimental results and demonstrate its performance under several type of datasets and settings, a variety of remote sensing data has been selected with different spatial and spectral characteristics. In the following

sub-sections, the developed method was compared against previous research efforts (Tzotsos et al., 2011) and other standard OBIA implementations implemented in Orfeo Toolbox (Inglada and Christophe, 2009).

4.1. Very high spatial resolution airborne imagery

The developed methodology was applied to a variety of very high and ultra high resolution remote sensing imagery. At first a 5cm resolution image from a DMC airborne digital scanner was tested. This kind of data is practically impossible to handle using traditional pixel-based classification and image analysis approaches. As shown in Fig.2 it is possible to segment this image into primitive objects in order to construct a feature space for OBIA classification. In this figure, a comparison of various segmentation methods is performed. Initially, the standard MSEG segmentation algorithm is tested in (a) at a scale of 100. The MSEG algorithm is applied on a scale-space AML representation and the result is achieved without any parameter tuning.

In Fig.2 (d) results from the application of the developed edge-constrained MSEG algorithm are demonstrated. The edge objects are not merged to the rest of the image objects and they remain unmerged until a final step concludes the segmentation procedure and produces the result in Fig. 2e. A comparison of the proposed algorithm with Mean-Shift algorithm (Fig.2 b) shows that while in some image regions Mean Shift can merge large parts of the image into one object, it fails to do so in other areas of the same texture. This behavior is not optimal and can lead to problems for classification steps since the mean object size varies. On the other hand Watershed segmentation (Fig.2 c) manages to segment the image with a homogeneous object size, but it suffers from major over-segmentation problems. For both algorithms the

default values were used to avoid parameter tuning. The proposed method on the other side (Fig.2 e,f), manages to obtain similar objects in size, which can be very applicable in a multiscale OBIA approach to classification. The main difference between (Fig. 2e) and (Fig. 2f) is that image edges are larger in number as derived from the Canny algorithm and this leads to better results, in areas that LSD (Fig. 2f) has not detected any straight lines in the image. So the LSD method is not very suitable for curved or small edges.

In order to evaluate the proposed method and to show the advantages of edge-constrained segmentation algorithm, a test similar to the one performed in (Tzotsos et al., 2011) was deployed. For this test a very high resolution aerial scanner image was used with 4 spectral bands, in order to perform full scale Object-Based Image Analysis tests. The initial image was segmented using a simple MSEG algorithm, without parameter tuning (default values of scale parameter 100, color 0.8 and shape 0.2 were selected). After primitive objects were obtained, a training set was given to a kernel-based classifier (SVM) to perform learning, based on the feature space introduced by object spectral and shape properties. For this test four generic land cover classes were used: Vegetation, Tile Roofs, Bright Roofs and Asphalt like materials. A set of training samples/objects was introduced to the SVM and a classification was performed. Using ground truth data, a quantitative evaluation was performed and a confusion matrix is presented in Table 1. The accuracy of the object-based classification was 88.07% similar to the results reported for this approach in (Tzotsos and Argialas, 2008).

A similar approach was then followed for the same image, with the same segmentation parameters and the same training and testing samples. This

time, a scale-space AML representation was used to provide anisotropic diffusion and simplification of the initial dataset. After SVM classification and evaluation of results (Table 1) an overall accuracy of 89.29% was achieved. similar to the accuracy reported in (Tzotsos et al., 2011).

Finally the proposed method was applied in a similar manner to the same data. A scale-space AML method was used to simplify the initial dataset. A segmentation step was then performed using the edge-constrained MSEG algorithm, and specifically the Canny edge features option was used. A set of primitive objects was obtained and object properties were extracted (spectral and shape features). The same training test was given to the SVM classifier and a finale classification of objects was obtained. As shown in Table 1, the overall accuracy of the proposed method, outperformed the previous tests with an accuracy of 90.29%. This shows that edge features helped the segmentation procedure to obtain more meaningful objects, that are capable of providing very good classification results. This procedure was repeated again with some different parameters and similar results were produced. Of course the difference in accuracy is not wide, but it is a measure that compatible results are produced for further OBIA classification steps.

4.2. Radar satellite imagery

Experimental results includes the application of the developed methodology at high resolution SAR data (TerraSAR-X dataset). The initial SAR image is shown in Fig. 3 (a) and the output result from the edge-constrained segmentation are compared with the ones from the Mean-Shift and Watershed Fig. 3 (b and c). The Mean-Shift method did not perform well, and resulted in under-segmentation of the shore line (Fig 3b). Even if the water area

was successfully segmented into one image object, the under-segmentation is always a very poor image segmentation performance. The applications the Watershed algorithm (Fig 3c), on the other hand, resulted in serious over-segmentation as can be seen in Figure 3.

A better result was obtained with the application of the standard MSEG algorithm, although there were some problems in objects near the shore line (Fig 3e). For this reason a Canny edge feature extraction was performed (Fig 3d) and the results were imported to the edge-constrained segmentation algorithm, which outperformed all other segmentation algorithms (Fig. 3f). The proposed algorithm managed to obtain image objects of similar scale and due to the imposed edge information the output boundaries describe clearly and more compact image objects. Again no parameter tuning was performed and default value of scale parameter 100 was used.

4.3. Multispectral remote sensing data

The next series of tests were performed on medium and high spatial resolution multispectral remote sensing data. For this, a Landsat TM image with pixel spatial resolution of 30m was used, as well as an QuickBird satellite image with 1m ground resolution and four spectral bands.

For the Landsat TM imagery, the same comparison of image segmentation methods was performed and is presented in Fig.4. In this situation the image had a stripping noise problem, making it more difficult for the segmentation algorithms to perform well. The application of MSEG with scale parameter 100 resulted in major over-segmentation, but still the algorithm resulted in objects similar in size and scale. The stripes of the image are obvious in this segmentation result (Fig.4a).

Mean-Shift segmentation algorithm performs much better in this specific test (Fig. 4b), since strong simplification of the image is involved internally, making the algorithm more robust in noise presence. On the other hand, still the size of image objects is variant across the image, even for the same semantic objects/areas. Watershed segmentation produced over-segmented results in this case too (Fig. 4c). A Canny edge detection step (Fig. 4d) was involved and the edge-constrained segmentation was tested (Fig.4e). One can observe that the later produces much better results than the standard MSEG algorithm. Object boundaries are more clear and compact, while the mean size of the primitive objects is approximately the same across the image. A test was also performed with an increased scale parameter (Fig.4f). The developed edge-constrained segmentation performed even better at larger scales, while the stripping problem was less apparent (Fig.4f).

For the QuickBird imagery a similar test was performed and demonstrated at Fig.5 (e and h) within a semi-urban area. The proposed algorithm was able to detect building objects (Fig.5 g,h) and in particular when it was constrained by the LSP features (the scale parameter for the simplification was 400). Again similar problems occurred with the Mean-Shift algorithm (Fig.5b) obtaining objects at different scales (i.e larger objects in low contrast areas of the image). Watershed algorithm on the other hand, produced an over-segmentation (Fig.5c) but kept all image objects on the same scale. Both enhanced MSEG and Mean-Shift had good results in building objects with the proposed method having a small advantage in preserving the edges of the image semantics.

4.4. Hyperspectral remote sensing data

The proposed segmentation algorithm was also tested with hyperspectral remote sensing data, obtained by a CASI aerial scanner (Fig.6). The spectral resolution of the dataset was 95 bands and the spatial resolution was 5m. Again, mean-shift and watershed algorithms were tested to compare with the proposed method, but in this specific test, it was impossible for those algorithms to be applied to the full spectral resolution of the hyperspectral dataset, since both algorithms are not designed to work on a large number of image bands. For this test, a subset of bands were used to derive mean-shift and watershed results (Fig.6 b,c). Both those algorithms produced similar results for this test. A mixture of small scaled and large scaled objects were obtained at the same time, with watershed being more accurate in this case, providing better results in edge areas (Fig.6c).

On the other hand, MSEG is designed to be applied to images of any spectral resolution, up to 65535 bands. It is demonstrated in Fig.6d that the simple MSEG algorithm is performing very well, given that the default scale parameter is easily reached (since it is a heterogeneity threshold) with a big number of bands contributing to object heterogeneity. Therefore, this over-segmentation (Fig.6d) cannot be considered as a major problem, rather than an effect caused by the nature of this dataset. After application of a strong simplification AML filtering, the results were improved (Fig.6e). In all cases of MSEG application it is shown that MSEG respects the scale of the image objects in a better way that the other algorithms tested. This is very crucial for OBIA applications, especially when multiscale approaches are necessary. Finally the enhanced MSEG algorithm was tested in Fig.6f and the results

were obviously better that other approaches shown here. Edge information was preserved (Fig.6f) and size of the image objects still is similar for all objects on this scale.

5. Conclusions and Future Perspectives

A new object-based image analysis framework was proposed in this research, based on advanced edge features incorporated in a multiscale region merging algorithm. Advanced scale-space representations were used in order to avoid tuning of segmentation and feature extraction parameters, and kernel-based classification was implemented to complete the OBIA framework. The proposed image segmentation algorithm was shown to work on any type of remote sensing data, outperforming some widely used segmentation algorithms in some cases. The improvement of the MSEG segmantation results was demonstrated, and the edge enhancements were shown to make the algorithm robust and generic for multiscale OBIA applications. The performed qualitative and quantitative evaluation reported that the developed algorithm outperformed previous efforts, both regarding the construction of the object representations and the classification results. Some of the topics for further research and development are: solutions for object-specific extraction tasks based on the developed framework, and adaptation of the proposed methodology to specific remote sensing applications.

References

Akcay, H., Aksoy, S., 2008. Automatic detection of geospatial objects using multiple hierarchical segmentations. Geoscience and Remote Sensing,

IEEE Transactions on 46, 2097 –2111.

Aplin, P., Smith, G., 2008. Advances in object-based image classification. Interanational Archive of Photogrammetry, Remote Sensing and Spatial Information Sciences 37 (Part B7), 725–728.

Baatz, M., Schape, A., 2000. Multiresolution segmentation an optimization approach for high quality multi-scale image segmentation, in: Strobl, J. et al. (eds.): Angewandte Geographische Infor-mationsverarbeitung XII., Wichmann, Heidelberg. pp. 12–23.

Benz, U., Hofmann, P., Willhauck, G., Lingenfelder, I., Heynen, M., 2004. Multi-resolution, object-oriented fuzzy analysis of remote sensing data for gis ready information. ISPRS Journal of Photogrammetry and Remote Sensing 58 (3-4), 239–258.

Blaschke, T., 2010. Object based image analysis for remote sensing. ISPRS Journal of Photogrammetry and Remote Sensing 65 (1), 2–16.

Blaschke, T., Burnett, C., Pekkarinen, A., 2004. Image segmentation methods for object-based analysis and classification, in: de Jong, S.M., van der Meer, F.D. (Eds.), Remote Sensing and Digital Image Analysis: Including the Spatial Domain (Chapter 12), Kluwer Academic Publishers. pp. 211–236.

Blaschke, T., Hay, G., 2001. Object-oriented image analysis and scale-space: theory and methods for modeling and evaluating multi-scale landscape structure. Interanational Archive of Photogrammetry and Remote Sensing 34 (Part 4/W5), 22–29.

Blaschke, T., Lang, S., Hay, G., 2008. Object Based Image Analysis - Spatial concepts for knowledge driven remote sensing applications. New York: Springer.

Camps-valls, G., Bruzzone, L., 2005. Kernel-based methods for hyperspectral image classification. IEEE Transactions on Geoscience and Remote Sensing 43 (6), 1351–1362.

Canny, J., 1986. A computational approach to edge detection. Pattern Analysis and Machine Intelligence, IEEE Transactions on , 679–698.

Carleer, A., Debeir, O., Wolff, E., 2005. Assessment of very high spatial resolution satellite image segmentations. Photogrammetric Engineering and Remote Sensing 71 (11), 1285–1294.

Chia, A.Y.S., Rajan, D., Leung, M.K., Rahardja, S., 2012. Object recognition by discriminative combinations of line segments, ellipses, and appearance features. Pattern Analysis and Machine Intelligence, IEEE Transactions on 34, 1758 –1772.

Christophe, E., Inglada, J., 2009. Open source remote sensing: Increasing the usability of cutting-edge algorithms. IEEE Geoscience and Remote Sensing Newsletter.

Cufi, X., Munoz, X., Freixenet, J., Marti, J., 2003. A review of image segmentation techniques integrating region and boundary information. Advances in imaging and electron physics 120, 1–39.

Derrode, S., Mercier, G., 2007. Unsupervised multiscale oil slick segmentation

from sar images using a vector hmc model. Pattern Recognition 40, 1135–1147.

Doxani, G., Karantzalos, K., Tsakiri-Strati, M., 2012. Monitoring urban changes based on scale-space filtering and object-oriented classification. International Journal of Applied Earth Observation and Geoinformation 15, 38 – 48.

Dragut, L., Schauppenlehner, T., Muhar, A., Strobl, J., Blaschke, T., 2009. Optimization of scale and parametrization for terrain segmentation: An application to soil-landscape modeling. Computers & Geosciences 35 (9), 1875–1883.

Duarte-Carvajalino, J., Castillo, P., Vélez-Reyes, M., 2007. Comparative study of semi-implicit schemes for nonlinear diffusion in hyperspectral imagery. IEEE Transactions on Image Processing 16 (5), 1303–1314.

Duarte-Carvajalino, J., Sapiro, G., Vélez-Reyes, M., Castillo, P., 2008. Multiscale representation and segmentation of hyperspectral imagery using geometric partial differential equations and algebraic multigrid. IEEE Transactions on Geoscience and Remote Sensing 46 (8), 2418–2434.

Gilboa, G., 2008. Nonlinear scale space with spatially varying stopping time. Pattern Analysis and Machine Intelligence, IEEE Transactions on 30, 2175 –2187.

Hall, O., Hay, G.J., 2003. A multiscale object-specific approach to digital change detection. International Journal of Applied Earth Observation and Geoinformation 4 (4), 311–327.

Hay, G., Blaschke, T., Marceau, D., Bouchard, A., 2003. A comparison of three image-object methods for the multiscale analysis of landscape structure. ISPRS Journal of Photogrammetry and Remote Sensing 57 (5-6), 327–345.

Hay, G., Castilla, G., 2006. Object-based image analysis: Strengths, weaknesses, opportunities and threats. Interanational Archive of Photogrammetry, Remote Sensing and Spatial Information Sciences 36 (4/C42), on CD–ROM.

Hay, G., Castilla, G., Wulder, M., Ruiz, J., 2005. An automated object-based approach for the multiscale image segmentation of forest scenes. International Journal of Applied Earth Observation and Geoinformation 7 (4), 339–359.

Hay, G.J., Dub, P., Bouchard, A., Marceau, D.J., 2002. A scale-space primer for exploring and quantifying complex landscapes. Ecological Modelling 153 (1-2), 27 – 49.

Hofmann, P., Strobl, J., Blaschke, T., 2008. A method for adapting global image segmentation methods to images of different resolutions, in: International Conference on Geographic Object-Based Image Analysis. ISPRS Volume 38 (on CD-ROM).

Hsu, C.W., Lin, C.J., 2002. A comparison of methods for multiclass support vector machines. IEEE Transactions On Neural Networks 13 (2), 415–425.

Inglada, J., Christophe, E., 2009. The orfeo toolbox remote sensing image

processing software, in: Geoscience and Remote Sensing Symposium, 2009 IEEE International, IGARSS 2009, IEEE. pp. IV–733.

Jiang, H., Yu, S., Martin, D., 2011. Linear scale and rotation invariant matching. Pattern Analysis and Machine Intelligence, IEEE Transactions on 33, 1339 –1355.

Jimenez, L.O., Rivera-Medina, J.L., Rodriguez-Diaz, E., Arzuaga-Cruz, E., Ramirez-Velez, M., 2005. Integration of spatial and spectral information by means of unsupervised extraction and classification for homogenous objects applied to multispectral and hyperspectral data. IEEE Transactions on Geoscience and Remote Sensing 43 (4), 844–851.

Jung, C., 2007. Unsupervised multiscale segmentation of color images. Pattern Recognition Letters 28, 523–533.

Karantzalos, K., Argialas, D., 2006. Improving edge detection and watershed segmentation with anisotropic diffusion and morphological levelings. International Journal of Remote Sensing 27 (24), 5427–5434.

Karantzalos, K., Argialas, D., Paragios, N., 2007. Comparing morphological levelings constrained by different markers, in: ISMM, G.Banon, et al. (eds), Mathematical Morphology and its Applications to Signal and Image Processing, pp. 113–124.

Kermad, C., Chehdi, K., 2002. Automatic image segmentation system through iterative edge-region co-operation. Image and Vision Computing 20, 541–555.

Kimmel, R., Zhang, C., Bronstein, A., Bronstein, M., 2011. Are mser features really interesting? Pattern Analysis and Machine Intelligence, IEEE Transactions on 33, 2316 –2320.

Klonus, S., Tomowski, D., Ehlers, M., Reinartz, P., Michel, U., 2012. Combined edge segment texture analysis for the detection of damaged buildings in crisis areas. Selected Topics in Applied Earth Observations and Remote Sensing, IEEE Journal of 5, 1118 –1128.

Koenderink, J., 1984. The structure of images. Biological Cybernetics 50 (5), 363–370.

Lehmann, G., 2008. Label object representation and manipulation with itk. Insight J , 1–34.

Lennon, M., Mercier, G., Hubert-Moy, L., 2002. Classification of hyperspectral images with nonlinear filtering and support vector machines, in: IEEE International Geoscience and Remote Sensing Symposium, pp. 1670–1672.

Lindeberg, T., 1994. Scale-Space Theory in Computer Vision. Kluwer Academic Publishers, Dordrecht.

Liu, Y., Guo, Q., Kelly, M., 2008. A framework of region-based spatial relations for non-overlapping features and its application in object based image analysis. ISPRS Journal of Photogrammetry and Remote Sensing 63 (4), 461 – 475.

Martha, T., Kerle, N., van Westen, C., Jetten, V., Kumar, K., 2011. Segment optimization and data-driven thresholding for knowledge-based landslide

detection by object-based image analysis. Geoscience and Remote Sensing, IEEE Transactions on 49, 4928 –4943.

Matheron, G., 1997. Les Nivellements. Technical Report. Centre de Morphologie Mathematique, France.

Meyer, F., 2004. Levelings, image simplification filters for segmentation. International Journal of Mathematical Imaging and Vision 20, 59–72.

Meyer, F., Maragos, P., 2000. Nonlinear scale-space representation with morphological levelings. Journal of Visual Communication and Image Representation 11, 245–265.

Meyer, Y., 1998. The Levelings, in: Mathematical Morphology and Its Applications to Image and Signal Processing, Kluwer Academic Publishers.

Mladinich, C., et al., 2010. An evaluation of object-oriented image analysis techniques to identify motorized vehicle effects in semi-arid to arid ecosystems of the american west. GIScience and Remote Sensing 47, 53–77.

Myint, S.W., Gober, P., Brazel, A., Grossman-Clarke, S., Weng, Q., 2011. Per-pixel vs. object-based classification of urban land cover extraction using high spatial resolution imagery. Remote Sensing of Environment 115, 1145 – 1161.

Neubert, M., Herold, H., Meinel, G., 2006. Evaluation of remote sensing image segmentation quality - further results and concepts. Interanational Archive of Photogrammetry, Remote Sensing and Spatial Information Sciences 36 (4/C42), 6p.

Ouma, Y., Josaphat, S., Tateishi, R., 2008. Multiscale remote sensing data segmentation and post-segmentation change detection based on logical modeling: Theoretical exposition and experimental results for forestland cover change analysis. Computers & Geosciences 34 (7), 715–737.

Papari, G., Petkov, N., 2011. Edge and line oriented contour detection: State of the art. Image and Vision Computing 29, 79 – 103.

Paragios, N., Chen, Y., Faugeras, O., 2005. Handbook of Mathematical Models of Computer Vision. Springer.

Pavlidis, T., Liow, Y., 1990. Integrating region growing and edge detection. Pattern Analysis and Machine Intelligence, IEEE Transactions on 12, 225–233.

Perona, P., Malik, J., 1990. Scale space and edge detection using anisotropic diffusion. IEEE Transactions on Pattern Analysis and Machine Intelligence 12 (7), 629–639.

Plaza, A., Benediktsson, J.A., Boardman, J., Brazile, J., Bruzzone, L., Camps-valls, G., Chanussot, J., Fauvel, M., Gamba, P., Gualtieri, A., Marconcini, M., Tilton, J., Trianni, G., 2009. Recent advances in techniques for hyperspectral image processing. Remote Sensing of Environment 113 (S1), S110–S122.

Serra, J., 2000. Connections for Sets and Functions. Fundamentae Informaticа 41, 147–186.

Stewart, S., Hay, G., Rosin, P., Wynn, T.J., 2004. Multiscale structure in sedimentary basins. Journal of Basin Research 16 (2), 183–197.

Theodoridis, S., Koutroumbas, K., 2003. Pattern Recognition. Elsevier Academic Press.

Tzotsos, A., Argialas, D., 2006. Mseg: A generic region-based multi-scale image segmentation algorithm for remote sensing imagery, in: Proceedings of ASPRS 2006 Annual Conference, Reno, Nevada, May 1-5, ASPRS p.(on CD-ROM).

Tzotsos, A., Argialas, D., 2008. Support Vector Machine Classification for Object-Based Image Analysis. In: Blaschke T., Lang S. and Hay G. (Eds.) Object Based Image Analysis - Spatial concepts for knowledge driven remote sensing applications, New York: Springer pp. 663-679.

Tzotsos, A., Iosifidis, C., Argialas, D., 2008. A hybrid texture-based and region-based multi-scale image segmentation algorithm. In: Blaschke T., Lang S. and Hay G. (Eds.) Object Based Image Analysis - Spatial concepts for knowledge driven remote sensing applications, New York: Springer pp. 221-237.

Tzotsos, A., Karantzalos, K., Argialas, D., 2011. Object-based image analysis through nonlinear scale-space filtering. ISPRS Journal of Photogrammetry and Remote Sensing 66, 2 – 16.

Vapnik, V., 1998. Statistical Learning Theory. John-Wiley and Sons, Inc.

Von Gioi, R., Jakubowicz, J., Morel, J., Randall, G., 2010. Lsd: A fast line segment detector with a false detection control. Pattern Analysis and Machine Intelligence, IEEE Transactions on 32, 722–732.

Von Gioi, R., Jakubowicz, J., Morel, J., Randall, G., 2012. LSD: a Line Segment Detector. Image Processing On Line .

Wang, H., Oliensis, J., 2010. Generalizing edge detection to contour detection for image segmentation. Computer Vision and Image Understanding 114, 731 – 744.

Weickert, J., 1998. Anisotropic Diffusion in Image Processing. ECMI Series, Teubner-Verlag, Stuttgart, Germany.

Weickert, J., Ishikawa, S., Imiya, A., 1999. Linear scale-space has first been proposed in Japan. Journal of Mathematical Imaging and Vision 10 (3), 237–252.

Witkin, A., 1983. Scale-space filtering, in: International Joint Conference on Artificial Intelligence, pp. 1019–1021.

Xu, Y., Huang, S., Ji, H., Fermüller, C., 2012. Scale-space texture description on sift-like textons. Computer Vision and Image Understanding 116, 999 – 1013.

Yu, P., Qin, A., Clausi, D., 2012. Unsupervised polarimetric sar image segmentation and classification using region growing with edge penalty. Geoscience and Remote Sensing, IEEE Transactions on 50, 1302 –1317.

Zhong, B., Ma, K.K., Liao, W., 2009. Scale-space behavior of planar-curve corners. Pattern Analysis and Machine Intelligence, IEEE Transactions on 31, 1517 –1524.

Zhou, W., Huang, G., Troy, A., Cadenasso, M., 2009. Object-based land cover classification of shaded areas in high spatial resolution imagery of urban areas: A comparison study. Remote Sensing of Environment 113 (8), 1769–1777.

Classification Accuracy with MSEG only				
	Vegetation	Tile Roofs	Bright Roofs	Asphalt Like
Vegetation	15247	0	0	2539
Tile Roofs	198	2856	15	2849
Bright Roofs	0	1	8362	2064
Asphalt Like	215	34	498	35612
Overall Accuracy: 88.07%				

Classification Accuracy with AML				
Vegetation	15523	0	0	2263
Tile Roofs	15	3764	124	2015
Bright Roofs	0	0	8389	2038
Asphalt Like	583	30	482	35264
Overall Accuracy: 89.29%				

Classification Accuracy with AML and Edge enhancement				
	Vegetation	Tile Roofs	Bright Roofs	Asphalt Like
Vegetation	15791	34	0	1961
Tile Roofs	244	4710	45	919
Bright Roofs	0	0	8311	2116
Asphalt Like	141	909	475	34834
Overall Accuracy: 90.29%				

Table 1: Quantitative results regarding the classification accuracy for a high spatial resolution airborne multispectral dataset. The proposed OBIA methodology scored better, indicating that the enhancement of MSEG with advanced edge features along with advanced scale space representation (AML) and the kernel classifier (SVM) outperforms earlier approaches.

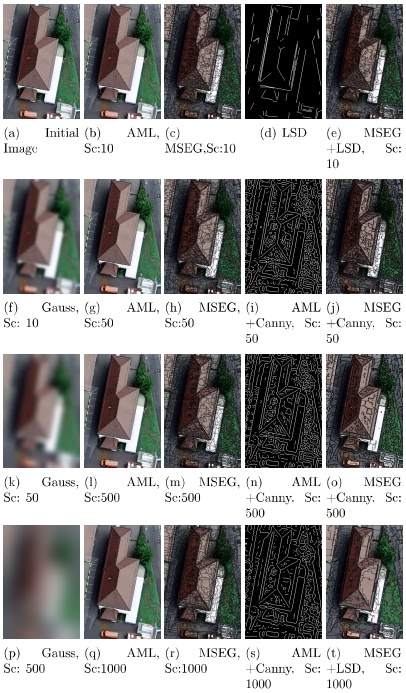

(a) Initial Image (b) AML, Sc:10 (c) MSEG,Sc:10 (d) LSD (e) MSEG +LSD, Sc: 10

(f) Gauss, Sc: 10 (g) AML, Sc:50 (h) MSEG, Sc:50 (i) AML +Canny, Sc: 50 (j) MSEG +Canny, Sc: 50

(k) Gauss, Sc: 50 (l) AML, Sc:500 (m) MSEG, Sc:500 (n) AML +Canny, Sc: 500 (o) MSEG +Canny, Sc: 500

(p) Gauss, Sc: 500 (q) AML, Sc:1000 (r) MSEG, Sc:1000 (s) AML +Canny, Sc: 1000 (t) MSEG +LSD, Sc: 1000

Figure 1: Comparing region merging segmentation results using scale space representation and advanced edge features. Four scales from various steps of the proposed methodology are presented. The first column (a,f,k,p) presents the initial remote sensing aerial image with spatial resolution of 5cm, along with three gaussian scales. The second column (b,g,l,q) presents the scale-space representation at various selected scales. The third column (c,h,m,r) presents initial image objects using the MSEG algorithm applied to the scale-space representation. The forth column (d, i ,n ,s) presents the advanced edge and line features used in the following step. The final column (e,j,o,t) shows the results of the edge enhanced MSEG algorithm proposed in this research.

(a) Standard MSEG (b) Mean-Shift (c) Watershed

(d) Edge MSEG, no merge of edge objects (e) Edge MSEG Canny (f) Edge MSEG LSD

Figure 2: Comparing various segmentation algorithms on a DMC aerial multispectral image with 5 cm pixel size (©Intergraph Corp.). (a) Standard MSEG with scale parameter 100. (b) Mean-Shift segmantation with default parameters. (c) Watershed segmentation with default parameters. (d) Edge constrained MSEG, without merging the edge objects in last pass, for demonstration purposes (e) Edge constrained MSEG, with Canny edge features used. (f) Edge constrained MSEG, with LSD edge features used.

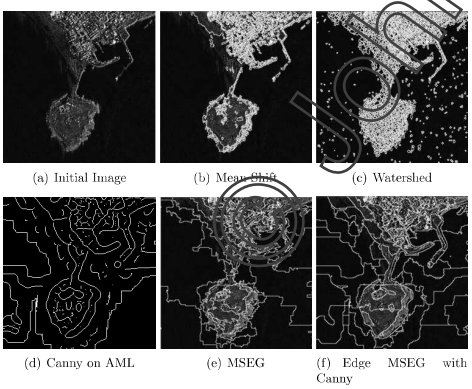

(a) Initial Image (b) Mean-Shift (c) Watershed

(d) Canny on AML (e) MSEG (f) Edge MSEG with Canny

Figure 3: Comparing various segmentation algorithms on a TerraSAR-X (©DLR) dataset (3 meters ground resolution, StripMap mode, polarisation HH). (a) The initial image. (b) Mean-Shift segmantation with default parameters. (c) Watershed segmentation with default parameters. (d) Canny edge detection applied on the AML scale-space representation. (e) Standard MSEG results with scale parameter 400. (f) Edge constrained MSEG, with Canny edge features used.

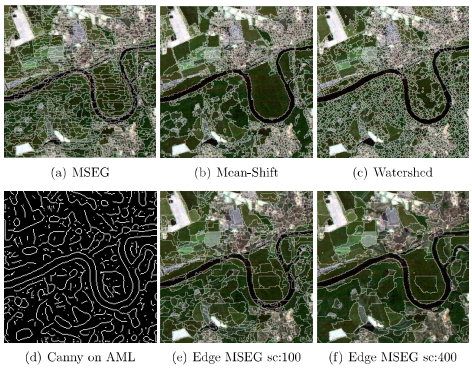

(a) MSEG (b) Mean-Shift (c) Watershed

(d) Canny on AML (e) Edge MSEG sc:100 (f) Edge MSEG sc:400

Figure 4: Comparing various segmentation algorithms on a Landsat TM dataset (Dessau, Germany). (a) Standard MSEG results with scale parameter 100. (b) Mean-Shift segmantation with default parameters. (c) Watershed segmentation with default parameters. (d) Canny edge detection applied on the AML scale-space representation. (e) Edge constrained MSEG, with Canny edge features used and scale parameter 100. (f) Edge constrained MSEG, with Canny edge features used and scale parameter 400.

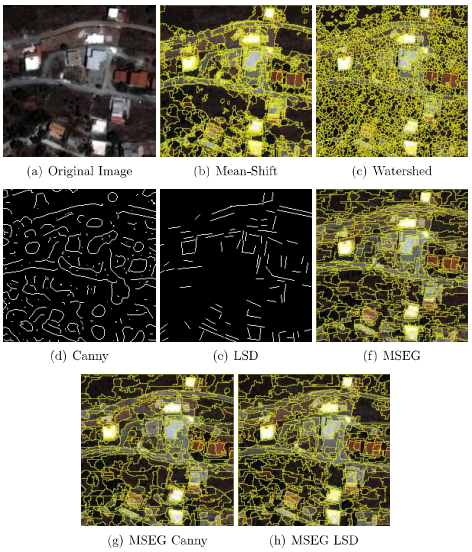

(a) Original Image (b) Mean-Shift (c) Watershed

(d) Canny (e) LSD (f) MSEG

(g) MSEG Canny (h) MSEG LSD

Figure 5: Comparing various segmentation algorithms on a QuickBird dataset (Eastern Attika, Greece). (a) Original image. (b) Mean-Shift segmantation with default parameters. (c) Watershed segmentation with default parameters. (d) Canny edge detection applied on the AML scale-space representation. (e) LSD line features extracted from the original image. (f) Standard MSEG results with scale parameter 100. (g) Edge constrained MSEG, with Canny edge features used and scale parameter 100. (h) Edge constrained MSEG, with LSD line features used and scale paramcter 100.

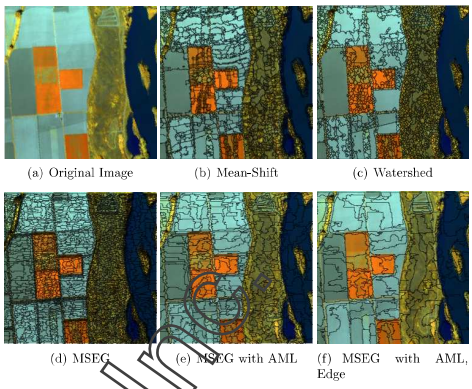

(a) Original Image (b) Mean-Shift (c) Watershed

(d) MSEG (e) MSEG with AML (f) MSEG with AML, Edge

Figure 6: Comparing various segmentation algorithms on a CASI Hyperspectral dataset (©Remote Sensing Laboratory, NTUA) with 95 spectral bands (Axios river, Thessaloniki, Greece). (a) Original image. (b) Mean-Shift segmantation with default parameters. (c) Watershed segmentation with default parameters. (d) Standard MSEG results with scale parameter 900. (e) Standard MSEG on AML scale-space representation and scale parameter 900. (f) Edge constrained MSEG, with Canny edge features used and scale parameter 900.